Summary

The styrene complexes of $M(NH_3)_5^{2+}$ (M^{II} = R^{II}, Os^{II}) and Ru^{II}(hedta)$^-$ have been shown to exhibit the same effects on the ^1H and ^{13}C NMR spectra as their linear olefin counterparts. The magnitudes of the upfield shifts for the protons in the coordinating olefin region are virtually the same for the respective Ru^{II} and Os^{II} complexes. The $E_{1/2}$ values of related members are nearly identical with those of linear olefins and diene cases where conjugation is small. Therefore the exo olefinic region is the preferential site of addition for A_5Ru^{2+}, A_5Os^{2+}, or Ru^{II}(hedta)$^-$; almost no influence on the electrochemical potential is observed by a change in the para substituent of the aromatic ring from -H to -COOH or $-CO_2^-$. This provides additional evidence for insulation of the olefin moiety of styrene from the phenyl ring. The A_5Os^{2+} case does exhibit evidence through its altered ^{13}C NMR spectrum of the carbon attached to the vinylic substituent for a greater interaction with Os^{II} in its $(NH_3)_5Os$(styrene)$^{2+}$ complex than for $(NH_3)_5Ru$(styrene)$^{2+}$. This has been tentatively expressed as a "more allylic-like" coordination of A_5Os^{2+} to styrene. The pentaamine environment was shown to be more able to compensate the ruthenium center compared to a polyamino polycarboxylate environment (hedta^{3-}) upon demand of a π-acceptor ligand. This is shown by an increase in $\Delta E_{1/2}$ as a function of the relative π-acceptor power of ligands as calibrated by the ESCA studies of Shepherd et al.[2] In this manner linear olefins, cyclic nonconjugated olefins, and styrenes are found to be normal π-acceptors. However acetylenes, with the DMAD complex used as a representative case, show high capacity as a π acceptor, but upon electronic demand, as in the Ru(hedta)(DMAD)$^-$ complex, the same group can synergistically π donate. This makes the $E_{1/2}$ value of Ru(hedta)(DMAD)$^-$ much closer to the $(NH_3)_5Ru$-(DMAD)$^{2+}$ value even though DMAD is a strong π acceptor on the ESCA scale.

Acknowledgment. We gratefully acknowledge support of this research through grants by the donors of the Petroleum Research Fund, administered by the American Chemical Society, and by the National Science Foundation (CHE-84417751).

(36) Holl, L. A.; Shepherd, R. E. To be submitted for publication in *Inorg. Chim. Acta.*

Contribution from the Laboratoire de Chimie Théorique, Université de Paris-Sud, 91405 Orsay, France, Laboratoire de Spectrochimie des Eléments de Transition, Université de Paris-Sud, 91405 Orsay, France, and Department of Chemistry, North Carolina State University, Raleigh, North Carolina 27695-8204

Energy Factors Governing the Partial Irreversibility of Lithium Intercalation in Layered Trichalcogenides MX_3 (M = Ti, Zr, Hf; X = S, Se) and the Structural Changes in the Intercalated Species Li_3MX_3

Enric Canadell,*[†] Claudine Thieffry,[†] Yves Mathey,*[‡] and Myung-Hwan Whangbo*[§]

Received November 21, 1988

The two-step mechanism proposed to explain the results of electrochemical intercalation of layered trichalcogenides MX_3 (M = Ti, Zr, Hf; X = S, Se) cannot explain the results of chemical intercalation. Thus, we propose a one-step mechanism for chemical intercalation in which each metal of MX_3 is affected by three lithium atoms at a time and analyze the merits of the one- and two-step mechanisms. State correlation diagrams show that the one- and two-step mechanisms are symmetry-allowed and symmetry-forbidden, respectively. This conclusion is supported by tight-binding band electronic structure calculations on the model ZrS_5 chain. The cell parameter changes from *a*, *b*, and *c* in MX_3 to approximately $2a + 1$, *b*, and $c + 0.3$ in Li_3MX_3 are explained by considering how the X-X bond breaking affects the interchain X···X and M···X interactions.

Layered transition-metal trichalcogenides MX_3 (M = Ti, Zr, Hf; X = S, Se)[1] consist of MX_3 slabs held together by van der Waals forces as schematically shown in **1** and **2**. Each MX_3 slab

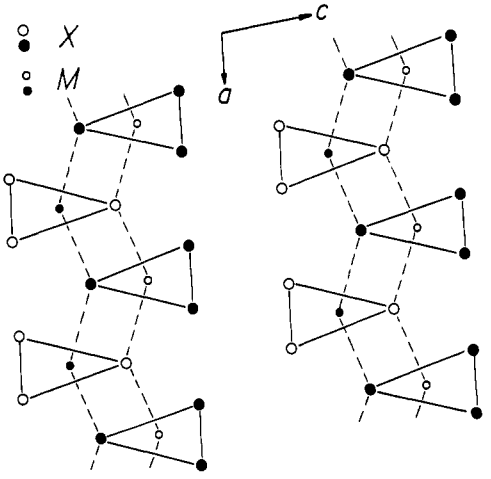

1

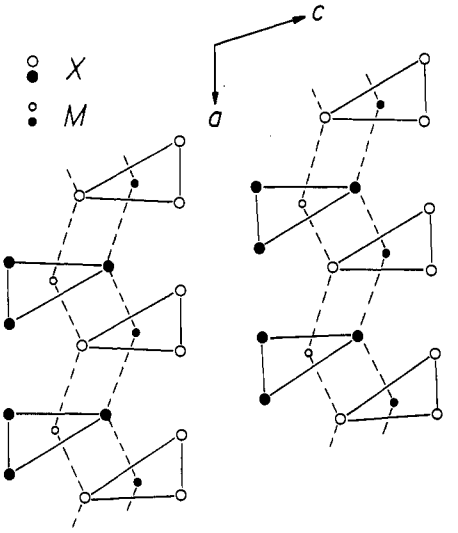

2

is made up of trigonal-prismatic MX_3 chains in such a way that two rectangular faces of an MX_6 prism are capped by X atoms of neighboring MX_3 chains. As a result, each metal atom M is coordinated to eight X atoms as shown in **3a**. Layered tri-

[†] Laboratoire de Chimie Théorique, Université de Paris-Sud.
[‡] Laboratorie de Spectrochimie des Eléments de Transition, Université de Paris-Sud. Present address: Département de Physique, Faculté de Sciences de Luminy, 13288 Marseille, France.
[§] North Carolina State University.

(1) Furuseth, S.; Brattas, L.; Kjekshus, A. *Acta Chem. Scand.* **1975**, *A29*, 623.

0020-1669/89/1328-3043$01.50/0

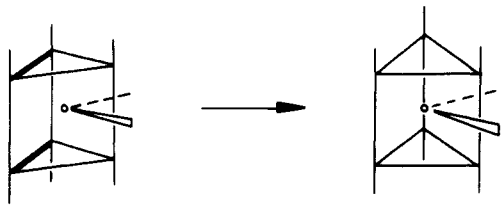

3a 3b

chalcogenides MX_3 have two structural variations, types A and B shown in **1** and **2**, respectively. The triangular face of an MX_6 prism is nearly symmetric in type A and is strongly asymmetric in type B. Short interchain M···X and X···X contacts are present in both type A and B structures. According to the formal oxidation state $(M^{4+})(X_2^{2-})(X^{2-})$ for MX_3, the metal electron counting is d^0 so that both type A and type B MX_3 are semiconductors. However, type B MX_3 has a smaller band gap than does type A MX_3 due to the shorter interchain X···X contacts in the former.[2]

MX_3 systems intercalate lithium atoms up to three Li atoms per MX_3 either by electrochemical or by chemical intercalation.[3,4] Important questions concerning the lithium intercalation of MX_3 are the reduction sites (e.g., metal M or X–X bonds), intercalation mechanisms, and lithium sites in the lattice. Results of electrochemical intercalation have been interpreted in terms of a two-step process:[4-6]

$$MX_3 + 2Li \rightarrow Li_2MX_3 \quad (1)$$

$$Li_2MX_3 + xLi \rightarrow Li_{2+x}MX_3 \quad (0 < x < 1) \quad (2)$$

The first stage is believed to break the X–X bonds of MX_3 (i.e., $X-X^{2-} + 2e^- \rightarrow 2X^{2-}$), and the second stage is believed to reduce the metal (i.e., $M^{4+} + xe^- \rightarrow M^{(4-x)+}$). Electrochemical intercalation and deintercalation studies of Li_xMX_3 show that the reaction is reversible only for $2 < x < 3$. The irreversibility for $0 < x < 2$ has been explained in terms of a structural change, from prismatic to octahedral coordination,[7] which the metal atom is presumed to undergo during the first stage of intercalation.

Chemical intercalation studies on MX_3 with *n*-butyllithium present quite a different picture of intercalation process. During intercalation of MX_3 with xLi ($x < 3$), there are always two phases Li_3MX_3 and MX_3, as if a metal atom is affected by three Li atoms at a time.[3,8,9] This observation cannot be explained in terms of the two-step process deduced from the electrochemical intercalation studies. According to powder diffraction studies on Li_3MX_3, the cell parameters (in Å) of Li_3MX_3 are approximately given by $2a + 1$, b, and $c + 0.3$, where a, b, and c are the cell parameters of MX_3. This observation[3] does not support the proposal of a prismatic-to-octahedral coordination change as a reason for the irreversibility of lithium intercalation for $0 < x < 2$ in Li_xMX_3, since doubling of the b-axis is not observed in Li_3MX_3. IR and Raman studies[9] on Li_3MX_3 show that lithium intercalation of MX_3 does indeed break the X–X bonds. In addition, they suggest that, as a result of intercalation, lithium atoms reside not only between the MX_3 slabs but also between the MX_3 chains within each MX_3 slab.[3,9]

The main objective of the present work is to examine why a metal atom M of MX_3 is affected by three Li atoms at a time and why the intercalation is reversible only for $2 < x < 3$ in Li_xMX_3. These questions are probed in terms of qualitative state-energy correlation diagrams for $2Li + MX_3 \rightarrow Li_2MX_3$ and $3Li + MX_3 \rightarrow Li_3MX_3$, which we construct on the basis of the X–X bond dissociation energy, the band gap of MX_3, and the tight-binding band electronic structure[10] of MX_3 calculated by using the extended Hückel method.[11] The atomic parameters employed in the calculations were taken from previous work.[2,12]

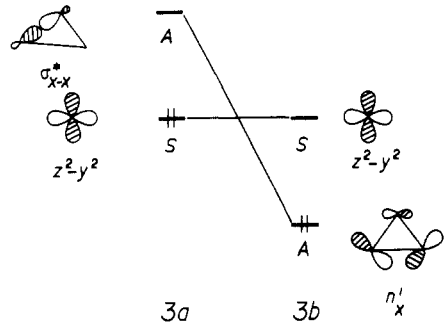

Figure 1. Simplified orbital correlation diagram for the distortion **3a** → **3b**, where the symmetry of the orbitals was classified with respect to the mirror plane of symmetry bisecting the X–X bond, which is broken during the distortion.

One-Step Intercalation Process

When the X–X bonds of the bicapped trigonal prism **3a** are broken, a new bicapped trigonal prism, **3b** is obtained. A simplified orbital correlation diagram for the structural change **3a** → **3b** is shown in Figure 1 (normalized to one MX_3 formula unit), where the $z^2 - y^2$ level is the lowest lying d-block level of MX_3, and other d-block levels lying below the σ_{X-X}^* level are not shown for simplicity (see Figure 2). The σ_{X-X}^* level of **3a** is converted to the lone-pair level n_x' of **3b** after the X–X bond breaking.[13] The energy levels of Figure 1 may be filled by two electrons to simulate the case of Li_2MX_3. Then the structural change **3a** → **3b** is a symmetry-forbidden reaction,[14] since the orbital symmetry of the $z^2 - y^2$ level differs from that of the σ_{X-X}^* or the n_X' level. This finding does not support the two-step intercalation process mentioned earlier. In a case when a metal atom of MX_3 is affected by three lithium atoms at a time (hereafter, referred to as a one-step intercalation process), the d-block levels of a given metal center are expected to receive three electrons released by three lithium atoms. For a one-step intercalation process to be correct, it is necessary that it not introduce symmetry-forbiddenness. In addition, it should be possible for a metal atom to accommodate three lithium atoms around it.

Acceptor Levels of MX_3

To construct a state correlation diagram for **3a** → **3b**, we need to know what kinds of acceptor levels each metal has in MX_3. Figure 2 shows the d-block levels of equilateral-triangular prism MX_6 (**4**), isosceles-triangular prism MX_6 (**5**), and bicapped isosceles-triangular prism MX_8 (**6**). The d-block level splitting

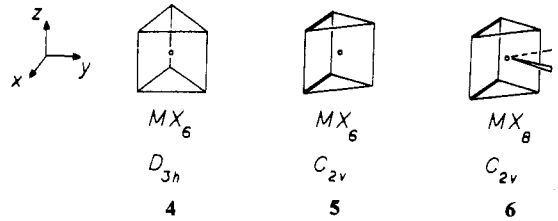

pattern of **4** is similar to that expected for octahedral MX_6.[15] The

(2) Canadell, E.; Mathey, Y.; Whangbo, M.-H. *J. Am. Chem. Soc.* **1988**, *110*, 104.
(3) Chianelli, R. R.; Dines, M. B. *Inorg. Chem.* **1975**, *14*, 2417.
(4) Whittingham, M. S. *J. Electrochem. Soc.* **1976**, *123*, 315.
(5) Jacobson, A. J. *Solid State* Ionics **1981**, *5*, 65.
(6) Whittingham, M. S. *Prog. Solid State Chem.* **1978**, *12*, 41.
(7) Murphy, D. W.; Trumbore, F. A. *J. Electrochem. Soc.* **1976**, *123*, 960.
(8) Mathey, Y., Unpublished results.
(9) Sourisseau, C.; Gwet, S. P.; Gard, P.; Mathey, Y. *J. Solid State Chem.* **1988**, *72*, 257.
(10) Whangbo, M.-H.; Hoffmann, R. *J. Am. Chem. Soc.* **1978**, *100*, 6093.
(11) Hoffmann, R. *J. Chem. Phys.* **1963**, *39*, 1397. A modified Wolfsberg–Helmholz formula was used to calculate the off-diagonal H_{ij} values. See: Ammeter, J. H.; Bürgi, H.-B.; Thibeault, J.; Hoffmann, R. *J. Am. Chem. Soc.* **1978**, *100*, 3686.
(12) Canadell, E.; Whangbo, M.-H. *Inorg. Chem.* **1978**, *26*, 3974.
(13) Hoffmann, R.; Shaik, S.; Scott, J. C.; Whangbo, M.-H.; Foshee, M. J. *J. Solid State Chem.* **1980**, *34*, 263.
(14) Woodward, R. B.; Hoffmann, R. *The Conservation of Orbital Symmetry*; Academic Press: New York, 1969.

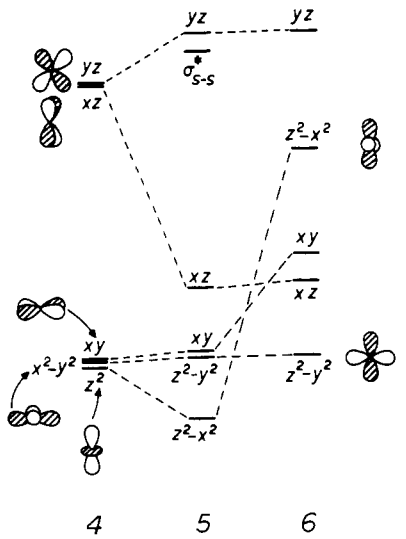

Figure 2. d-block levels of equilateral-triangular prism MX_6 (**4**), isosceles-triangular prism MX_6 (**5**), and bicapped isosceles-triangular prism MX_8 (**6**).

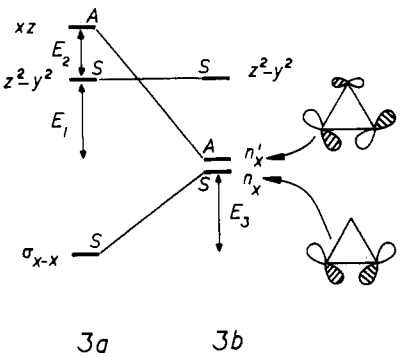

Figure 3. Orbital correlation diagram for the distortion **3a** → **3b**.

distortion **4** → **5** strongly lowers the xz level and slightly lowers the z^2 level, which is hybridized to become the $z^2 - x^2$ level in **5**. The $x^2 - y^2$ level of **4** is hybridized to become the $z^2 - y^2$ level of **5**. By introduction of the two capping X ligands to **5**, both $z^2 - x^2$ and xy levels are raised in energy beyond the $z^2 - y^2$ and xz levels, so that the latter become the two lowest lying levels of **6**. Thus, if a metal center of MX_3 receives three electrons, its electron configuration is likely to be $(z^2 - y^2)^2(xz)$. It is important to note that the xz level has the σ_{X-X}^* orbital character combined in phase with the metal xz orbital, as depicted in **7**. Thus, it is clear that, for the distortion **3a** → **3b**, the xz level of **3a** also correlates with the n_X' level of **3b**.

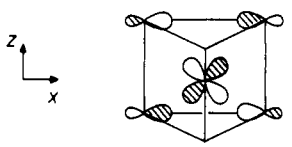

7

Orbitals Involved in X–X Bond Breaking

The previous section showed that the most likely acceptor levels of **3a** are the $z^2 - y^2$ and xz orbitals, which correlate with the $z^2 - y^2$ and n_X' levels of **3b**, respectively (see Figure 3). Another orbital of **3a** that is strongly affected by the X–X bond breaking is the X–X bonding level σ_{X-X}. This orbital correlates with the lone-pair level n_X of **3b** as shown in Figure 3. To construct a state correlation diagram for **3a** → **3b**, it is necessary to know the relative energies E_1, E_2, and E_3 of those levels defined in Figure 3. We estimate E_1, E_2, and E_3 by considering ZrS_3 as a representative example of MX_3 (i.e., X = S). Then, in Figure 3, E_3 is the energy difference between the S–S bonding (σ_{S-S}) and the sulfur lone-pair (n_S) levels. Thus, E_3 can be approximated by half the bond dissociation energy of a S–S single bond, which is 2.7 eV.[16] E_1 is the energy difference between the sulfur lone pair (n_S') and the lowest lying d-block level ($z^2 - y^2$). Thus, E_1 can be approximated by the optical energy gap of ZrS_3, which is greater than 2.1 eV.[17-19] We employ the most conservative choice, E_1 = 2.1 eV. E_2 is the energy difference between the xz and $z^2 - y^2$ levels. Since no experimental estimate for E_2 is available, we rely on our results of molecular orbital calculations on MS_8 cluster **6** (M = Ti, Zr). These calculations show that E_2 = 1.0 eV and is nearly independent of the valence-shell ionization potential chosen for the metal 3d orbital within 2 eV variation.

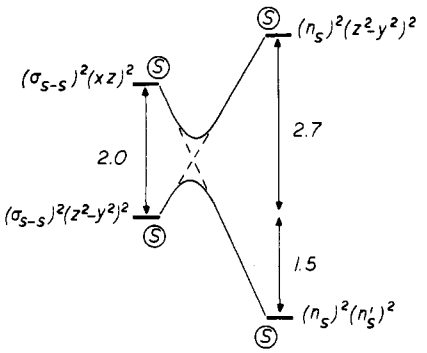

Figure 4. State correlation diagram of the two-lithium process for the distortion **3a** → **3b**, where the energy differences between the states are given in units of eV.

State Correlation Diagrams

We now construct state correlation diagrams for **3a** → **3b** on the basis of the relative energies E_1, E_2, and E_3 discussed in the previous section. Correlation diagrams of interest for us are those that simulate the following reactions:

$$2Li + MX_3 \rightarrow (Li^+)_2\, MX_3^{2-} \quad (3)$$

$$3Li + MX_3 \rightarrow (Li^+)_3\, MX_3^{3-} \quad (4)$$

Since lithium gives its valence electron to the MX_3 lattice, to the d-block levels of **3a** (see Figure 3), the "two-lithium" process (eq 3) gives two electrons, while the "three-lithium" process (eq 4) gives three electrons.

Figure 4 shows the state correlation diagram for the two-lithium process. In constructing this diagram, we assume that the X_3 triangles are isosceles and the mirror plane of symmetry bisecting the X–X bonds remains intact throughout the distortion **3a** → **3b**. As will be commented later, removal of this constraint does not change our conclusion. According to the orbital correlation diagram of Figure 3, the state $(\sigma_{S-S})^2(z^2 - y^2)^2$ and $(\sigma_{S-S})^2(xz)^2$ of **3a** are intended to correlate with the states $(n_S)^2(z^2 - y^2)^2$ and $(n_S)^2(n_S')^2$, respectively. All of these states are symmetric, so that there occurs a noncrossing of the energy surfaces, thereby leading to an energy barrier for the conversion **3a** → **3b**. As already noted, therefore, the two-lithium process is a symmetry-forbidden reaction.[16] Figure 5 shows the state correlation diagram for the three-lithium process. The states $(\sigma_{S-S})^2(z^2 - y^2)^2(xz)^1$ and $(\sigma_{S-S})^2(z^2 - y^2)^1(xz)^2$ of **3a** correlate with the $(n_S)^2(n_S')^1(z^2 - y^2)^2$ and $(n_S)^2(n_S')^2(z^2 - y^2)^1$, respectively. The two energy surfaces have different symmetries, so that they cross each other. In contrast to the case of the two-lithium process, the three-lithium process is exothermic and exhibits no activation barrier. As already present in type B MX_3 and, to a lesser extent, in type A MX_3 as well, real MX_3 does not consist of isosceles X_3 triangles. Therefore, removal of the miror plane of symmetry in the correlation diagram

(15) Albright, T. A.; Burdett, J. K.; Whangbo, M.-H. *Orbital Interactions in Chemistry*; Wiley: New York, 1985.

(16) Purcell, K. F.; Kotz, J. C. *Inorganic Chemistry*; W. B. Saunders: Philadelphia, 1977; p 270.

(17) Schairer, W.; Shafer, M. W. *Phys. Status Solidi A* **1973**, *17*, 181.

(18) Perluzzo, G.; Jandl, S.; Girard, P. E. *Can. J. Phys.* **1980**, *58*, 143.

(19) Nee, S. F.; Nee, T. W.; Fan, S. F.; Lynch, D. W. *Phys. Status Solidi B* **1982**, *113*, K5.

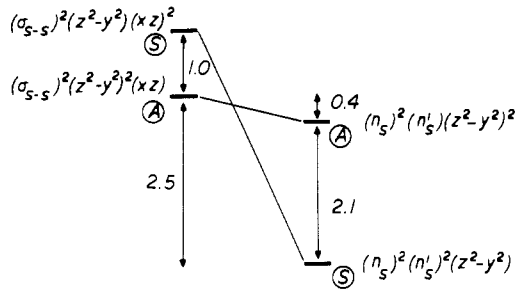

Figure 5. State correlation diagram of the three-lithium process for the distortion **3a** → **3b**, where the energy difference between the states are given in units of eV.

makes all the states of Figure 5 symmetric, which leads to a noncrossing of the two potential energy surfaces, thereby providing a strong driving force for the **3a** → **3b** conversion. Thus, the three-lithium process is a symmetry-allowed reaction.[14] This might be the reason why each metal atom of MX_3 is affected by three lithium atoms at a time during intercalation.

At the end of the three-lithium process, the $z^2 - y^2$ level of **3b** has one electron. This level is largely metal in character, so that removal of its electron would be easy since no significant geometry reorganization is necessary, and hence deintercalation of Li_xMX_3 would be reversible for $2 < x < 3$. Deintercalation of Li_3MX_3 beyond more than one lithium is expected to have a high activation energy barrier because such a process would lead to a symmetry-forbidden, strongly endothermic situation, as shown in **8** in

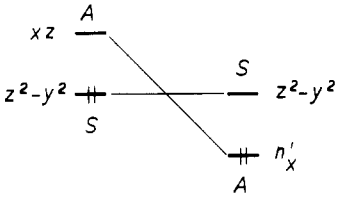

8

terms of orbital correlation diagram. These account for the irreversibility of intercalation in Li_xMX_3 for $x < 2$, and the reversibility of electrochemical intercalation in Li_xMX_3 for $2 < x < 3$.

To confirm the above conclusions derived from the qualitative state correlation diagrams, we carry out tight-binding band electronic structure calculations on a single ZrS_5 chain (i.e., a single ZrS_3 chain with two capping ligands S at each Zr) as a function of the S-S bond breaking. **9a** and **9b** are projection views

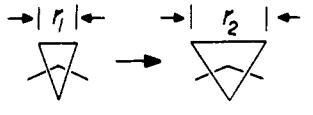

9a **9b**

of the ZrS_5 chains that represent **3a** and **3b**, respectively, where r_1 refers to the distance of the S–S bonds to be broken. In our calculations of the total electronic energies of **9**, the S–S bond distance was gradually increased from 2.09 Å in **9a** to 2.57 Å in **9b**. The extent of this S–S bond lengthening is the same as that of the Se–Se bond lengthening found in $NbSe_3$. [I.e., 2.57 = 2.09 × (2.91/2.37), where the Se–Se pair distances of 2.91 and 2.37 Å are the longest and the shortest ones, respectively, among the three different types of $NbSe_3$ chains in $NbSe_3$.[20] From the electronic viewpoint, the Se–Se pairs with the distances of 2.91 and 2.37 Å are described by $(Se^{2-})_2$ and $(Se_2)^{2-}$, respectively.[21]] Parts a and b of Figure 6 respectively show the potential-energy curves of the two- and three-lithium processes obtained by employing tight-binding band calculations on **9** as a function of r_1.

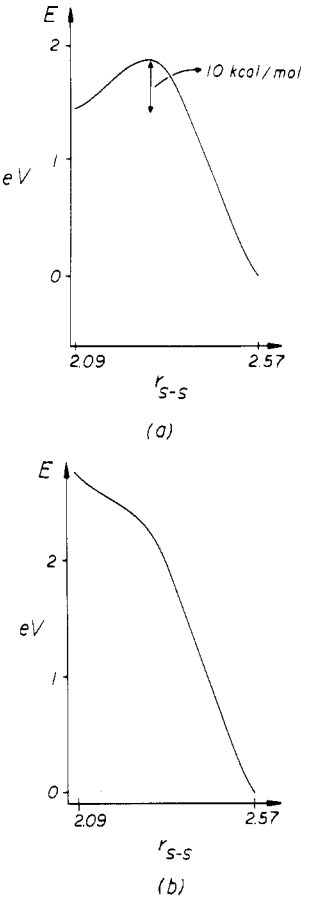

Figure 6. Calculated relative total electronic energies of the ZrS_5 chain as a function of the S–S distance for the two-lithium process (a) and for the three-lithium process (b), where the reference is the structure in which the S–S bond is broken.

Clearly, the two-lithium process shows an activation energy (~10 kcal/mol per metal), while the three-lithium process does not. These results are in support of our conclusions derived from the state correlation diagrams.

Effects of the X–X Bond Breaking on Interchain Interactions

Let us now consider how the X–X bond breaking in one chain of MX_3 might affect the interchain interactions associated with the interchain X···X and M···X contacts. As depicted in **10** and

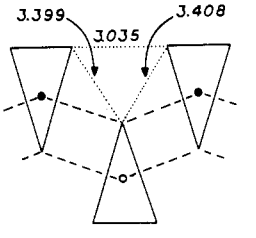

10

11 for ZrS_3 and TiS_3, respectively, the interchain X···X contacts

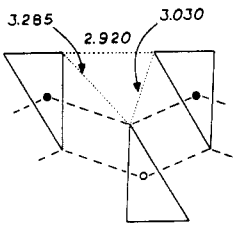

11

are short so that their nonbonded repulsions are not negligible. The X–X bond breaking would shorten the interchain X···X contacts thereby increasing the nonbonded repulsions, unless the

(20) Hodeau, J. L.; Marezio, M.; Roucau, C.; Ayroles, R.; Meerschaut, A.; Rouxel, J.; Monceau, P. *J. Phys. C.* **1978**, *11*, 4117.
(21) Whangbo, M.-H.; Gressier, P. *Inorg. Chem.* **1984**, *23*, 1305.

interchain M···X contact distances also increase to prevent the X···X contact distances from shortening. The interchain M···X interactions are stabilizing in nature and are primarily responsible for keeping the chains in a slab. Therefore, lengthening the M···X contacts is destabilizing, as is shortening the X···X contacts. Hence, the X-X bond breaking is opposed by the X···X nonbonded repulsion and by the M···X bonding. When these factors are taken into consideration, the activation barrier for the two-lithium process in Figure 6a becomes larger, and the exothermicity for the three-lithium process in Figure 6b becomes smaller. Namely, the conclusions derived from the state correlation diagrams of a single chain are not altered by including the effects of interchain interactions.

According to the trend in the Se–Se pair distances of $NbSe_3$ (vide supra), the X–X bond breaking is expected to increase the bond length by about 0.5 Å. Thus, if the interchain X···X contact distances remain constant, the X–X bond breaking would increase the *a* axis length by 0.5 Å. During the course of the X–X bond breaking, the expected increase in the nonbonded repulsions associated with the interchain X···X contacts can be reduced if every second prismatic chain slips out of the slab as shown in **12**. This

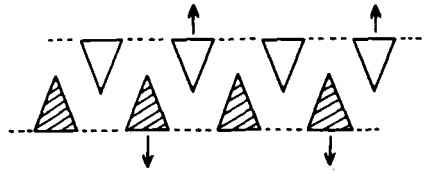

12

explains why lithium intercalation increases the *a* and *c* axis lengths to approximately $2a + 1$ and $c + 0.3$ Å, respectively.[3] The X–X bond breaking occurs in the *ac* plane, so that the *b* axis length is not affected by it, as observed experimentally.

That each metal atom is affected by three lithium atoms at a time during intercalation necessarily means that there are enough sites around each metal atom to accommodate three lithium atoms. Figure 7 shows tetrahedral sites around a single prismatic chain in ZrS_3. The sites A and A′ are shared by three chains, and the sites B and C, by two chains. Therefore, in average, each metal atom has five tetrahedral sites around it. Initially, the sites B and C may not be roomy enough, but the X–X bond breaking and the M···X distance lengthening would make those sites roomy. That is, each metal atom has more than enough sites to accommodate three lithium atoms around it. It is noted that two sites, A and A′, form a octahedral site. IR and Raman studies[9] of Li_3MX_3 are consistent with the view that, of three lithium atoms affecting a metal atom, one occupies an octahedral site while the other two occupy tetrahedral sites.

Concluding Remarks

Layered trichalcogenides MX_3 (M = Ti, Zr, Hf; X = S, Se) take up three lithium atoms per metal by electrochemical or chemical intercalation. Results of electrochemical intercalation have been explained in terms of a two-step mechanism. Since this mechanism cannot account for results of chemical intercalation, we proposed a one-step mechanism for chemical intercalation in which each metal atom is affected by three lithium atoms at a time. On the basis of ideal state correlation diagrams, the one- and two-step mechanisms are found to be symmetry-allowed and symmetry-forbidden, respectively. This observation is supported by tight-binding band electronic structure calculations. Thus, it is concluded that chemical lithium intercalation of MX_3 proceeds via the one-step mechanism. The cell parameter (in Å) changes from *a*, *b*, and *c* in MX_3 to approximately $2a + 1$, *b*, and $c + 0.3$ in Li_3MX_3 are easily explained by considering how the X–X bond breaking in each MX_3 chain affects the interchain X···X and M···X interactions. Each metal atom of MX_3 has five tetrahedral sites (or one octahedral and three tetrahedral sites), which are enough to accommodate three lithium atoms around each metal, thereby allowing the one-step mechanism to be operative.

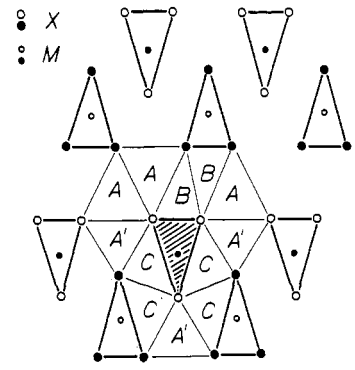

Figure 7. Tetrahedral sites around a single MX_3 chain in the MX_3 lattice.

Let us now briefly comment on the applicability of the one-step mechanism to electrochemical lithium intercalation of MX_3. Our work strongly suggests that a "two-electron" rupture of the X–X bond is energetically unfavorable, while a "three-electron" rupture of the X–X bond is energetically favorable. On the basis of this energetic argument, the plateau of the voltage discharge curve observed for electrochemical lithium intercalation of MX_3 needs to be associated with the presence of the two phases Li_3MX_3 and MX_3 rather than that of the two phases Li_2MX_3 and MX_3. The one-step mechanism predicts that electrochemical deintercalation in Li_3MX_3 is irreversible beyond more than one Li, in agreement with experiment. However, the one-step mechanism predicts the plateau of the voltage discharge curve to cover the lithium uptake region of zero to three Li atoms per MX_3 instead of zero to two Li atoms per MX_3 observed in the electrochemical intercalation studies.[4-6] Therefore, it seems that neither the one- or the two-step mechanism is totally satisfactory. Further studies are necessary to fully understand the electrochemical lithium intercalation behavior of MX_3.

Acknowledgment. Work at Université de Paris-Sud was in part supported by a grant from the Institut de Chimie Moleculaire d'Orsay (ICMO). Work at North Carolina State University was in part supported by the U.S. Department of Energy, Office of Basic Energy Sciences, Division of Materials Science, under Grant De-FG05-86ER45259.